JNC TN8400 2002－018

The Study of $^{105}Pd(n, \gamma)^{106}Pd$ Reaction with Thermal Neutrons

(Research Document)

July, 2002

TOKAI WORKS

JAPAN NUCLEAR CYCLE
DEVELOPMENT INSTITUTE

〒319－1184　茨城県那珂郡東海村村松4番地49
核燃料サイクル開発機構
技術展開部　技術協力課

Inquiries about copyright and reproduction should be addressed to :
Technical Cooperation Section,
Technology Management Division,
Japan Nuclear Cycle Development Institute
4-49 Muramatsu, Tokai-mura, Naka-gun, Ibaraki, 319-1184
Japan

Ⓣ

目次

1. Introduction

The palladium isotope ^{107}Pd is one of the long-lived (half-life 6.5×10^{6} yr)[1] fission products (LLFP) and it is important for the study of nuclear transmutation of radioactive waste. The neutron capture reaction is important for the study of nuclear transmutation. For the study of ^{107}Pd transmutation without isotope separation, the data for ^{105}Pd is also important; the nuclide ^{105}Pd absorb the thermal neutrons and affect the neutron field at target irradiation position. However, there is no experimental data so far on thermal neutron capture cross-sections of ^{105}Pd in the Exchange Format (EXFOR) data library except the evaluated data (20.25 barn)[2]. There is also no published paper on the cross section except the data at neutron resonance regions by Macklin *et al.*(1979). [3]

The γ-ray intensity (I_γ) is one of the fundamental quantities for deducing the cross-section from the γ-ray yields. However, there is no published data for I_γ of the product ^{106}Pd in the Evaluated Nuclear Structure Data File (ENSDF [4]). In order to obtain the reliable cross-section data for the reaction ^{105}Pd(n,γ)^{106}Pd, the partial level-scheme of ^{106}Pd was constructed and the γ-ray intensities (I_γ s) of the product were determined based on the level-scheme from the $\gamma-\gamma$ coincidence measurement.

2. Experimental

2.1 Irradiation of Samples

Samples of natural Pd and enriched ^{105}Pd together with Al foil were irradiated separately with the B-4 thermal neutron facility at Kyoto University Research Reactor Institute (KURRI). In each irradiation, the Al foil used as a neutron flux monitor was placed in such a way that the foil is always face in the beam direction. The prompt γ-rays have been measured using two high purity Ge detectors, and one of the detectors was surrounded by BGO spectrometer to suppress the Compton background for the irradiation of enriched ^{105}Pd

sample. The experimental arrangement for both cases has been shown in **Figure 1**. Moreover, the important characteristics of two irradiated samples with the corresponding monitor foils are shown below:

Sample: natural Pd target:

- shape: circular
- Purity : 99.99%
- Size : 0.6 cmϕ
- Weight : 43.2913±0.0001 mg
- Thickness: ~0.0125 cm
- Distance between the target to the end cap of the detector: 12.5 cm

Sample: enriched ^{105}Pd:

- Shape: rectangular,
- Enrichment: 93.8%
- Length: 2.0 cm, width: 1.0 cm,
- Thickness: ~ 0.00058 cm
- Weight: ~13.9099 ± 0.0001 mg
- Distance between the target to the end cap of the detector: 10 cm.

For Al monitor:

- Shape: circular
- Purity: 99.0%
- Size: 0.6 cm
- Weight: 17.7388±0.001 mg

For Al monitor:

- Shape: rectangular
- Length: 2.0 cm, width: 1.0 cm
- Thickness: 0.0118 cm
- Weight: 63.6 ± 0.1mg

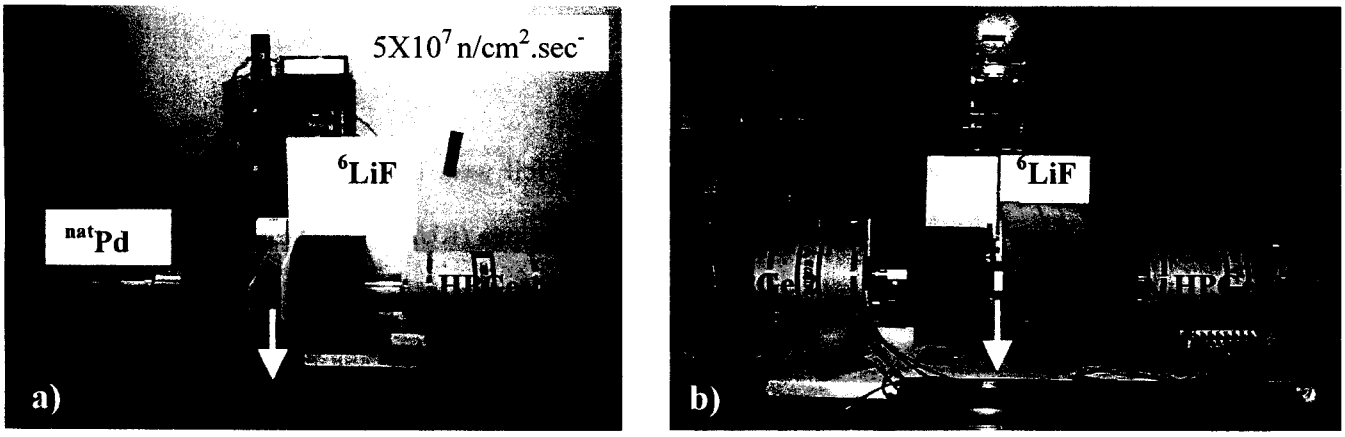

Fig. 1 The experimental arrangements for; a) natural Pd without BGO; b) Enriched ^{105}Pd with BGO

2.2 Data Acquisition

A brief schematic block diagram of data acquisition system is shown in **Figure 2.** Here, the system consisted of two high purity Ge detectors (HPGe 1 and 2) and a fast data acquisition system with some other electronic devices. The relative peak detection efficiency of each of two Ge detector is 90% (relative to a 7.62 x 7.62 cmϕ NaI) and the resolution of each detector (FWHM) is 2.5～2.8 keV at 1.33 MeV of ^{60}Co.

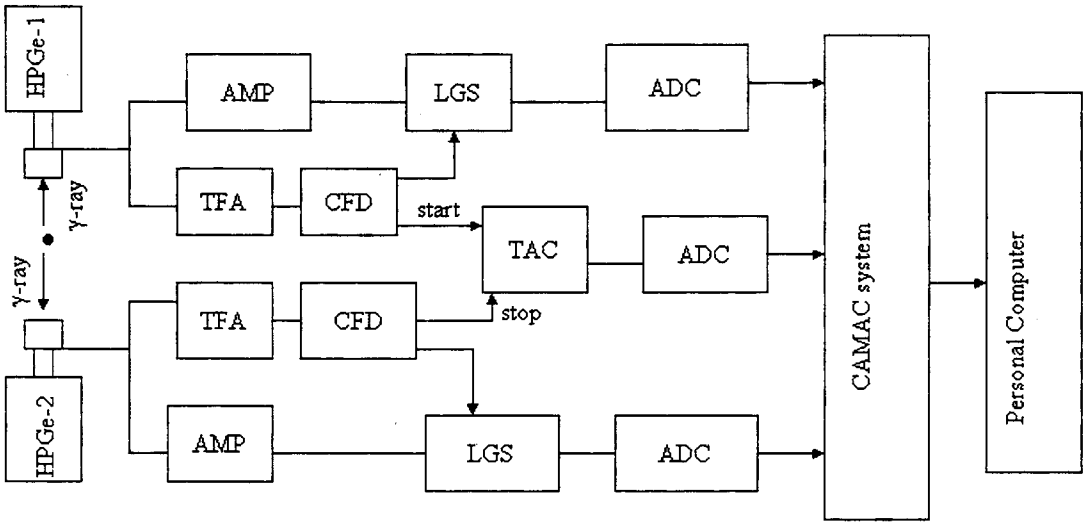

AMP: Amplifier LGS: Linear Gate and Stretcher; ADC: Analog to Digital Converter; TFA: Timing Filter Amplifier
CFD: Constant Fraction Discriminator; TAC: Time to Amplitude Converter;

Fig. 2 Schematic block diagram for the data acquisition system of $\gamma-\gamma$ coincidence measurement

The Ge preamplifier signals were fed into both a spectroscopy amplifier and a timing filter amplifier (TFA). The output of the spectroscopy amplifier provided the energy signal and converted to digital data using analog-to-digital converter (ADC). The outputs of TFA were connected to constant fraction discriminators (CFD) and the resulting signals from two detectors were used as a start and stop pulse for the time-to-amplitude converter (TAC). To reduce the dead times during the data acquisition, the event data are at first accumulated in one of

the two memory modules contained in the CAMAC system, which acts as a ring buffer and transferred the data to a personal computer. When such an action continues by the one memory module, while at the same time, the other one is active for data acquisition. At the end of the measurement, the accumulated data on PC were processed by off-line analysis.

3. Data Analysis

The data analysis can be grouped into:

- Analysis for the determination of relative γ-ray intensities, and
- Analysis for the determination of capture cross-section.

3.1 Determination of relative γ-ray intensities

The procedure for determining the relative γ-ray intensities involves: **i)** Determination of detector peak efficiency with necessary corrections, and **ii)** Measurement of peak areas of coincidence gated spectra.

i) Detector of peak efficiency

The energy and peak efficiency calibrations of the Ge detectors were performed using standard source ^{60}Co and γ-rays from ^{15}N produced via the reaction ^{14}N(n, γ)^{15}N. The absolute full energy peak efficiency was determined by using the standard point source ^{60}Co whose activity accuracy was 1.9% as the supplier of the source. In this determination, the correction for the contribution due to the coincidence-summing effect was made followed by the method [6] taking into account the angular correlations between cascading γ-rays derived by the relevant coefficient values from the literature (Ref.7, 8). A little more details regarding the same will be explained in the next section. The energy dependence relative peak efficiency was carried out from the

reaction $^{14}N(n, \gamma)^{15}N$ in the energy region from 1.67 to 8.31 MeV, whose γ-ray emission probability (I_γ) values were taken from the mean of experiments [9,10]. The single spectrum of the product ^{15}N for the mentioned reaction is shown in **Figure 3**.

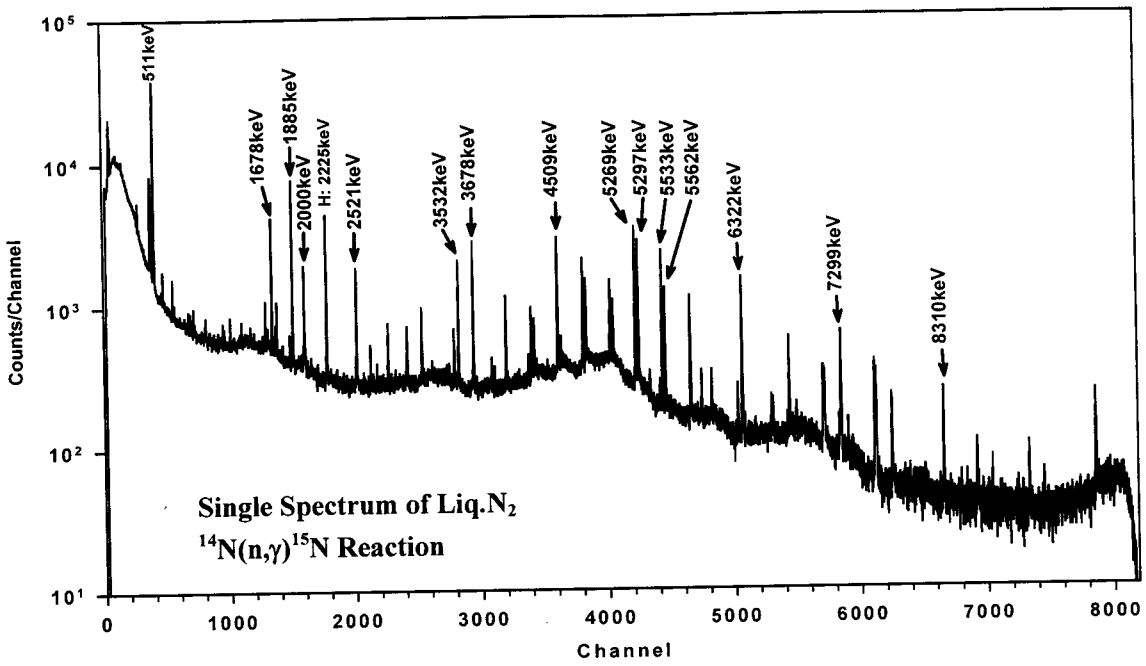

Fig. 3 Single spectrum of ^{15}N produced by the reaction $^{14}N(n,\gamma)^{15}N$

The relative efficiency curve was fitted by the following equation:

$$\varepsilon_{rel.} = \exp\{m_1 + m_2 * \ln(M_0)\} \quad (1)$$

where, m_1 and m_2 are normalization and slope parameters, respectively; M_0 is the γ-ray energy in MeV. The value of the slope parameter m_2 was taken from the relative efficiency curve fitting as shown in **Figure 4**. Right after then, by inserting the value of m_2 in the absolute peak efficiency at two energy points of ^{60}Co and the weighted mean of two was the normalization parameter value of m_1. The two determined parameters are: m_1= -5.2198 ± 0.01891, and m_2 = -0.92773 ± 0.011489; and hence the efficiencies at desired energies can be calculated by Eq. (1). However, the error of m_1 was chosen to equal or larger than the absolute efficiency of

the standard source ^{60}Co depending on the energy, which contributes according to the error propagation formula instead of the weighting errors. The efficiency of the detectors used for the irradiated enriched sample was carried out in the same manner as before and the parameters with errors are found to be: $m_2 = -0.8546 \pm 0.0038897$, and $m_1 = -4.7175 \pm 0.01919$.

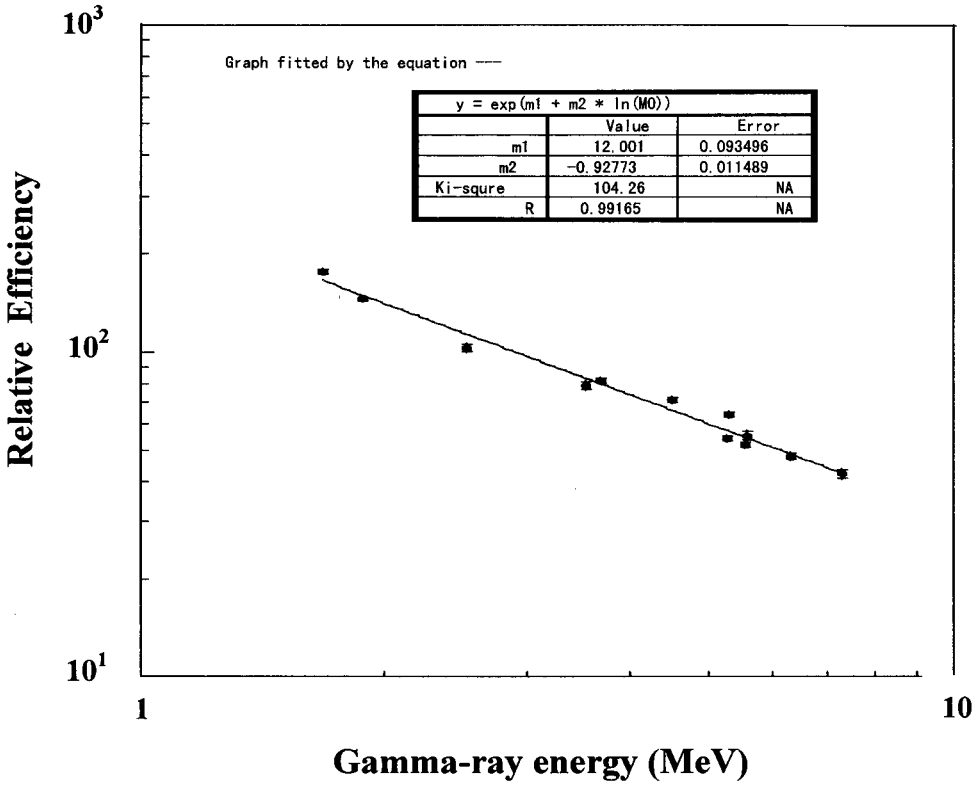

Fig. 4 Relative efficiency curve fitting for the reaction $^{14}N(n,\gamma)^{15}N$

3.2 Analysis of peak areas of coincidence gated spectra

Figure 5 shows the gates applied on γ-ray projection (singles) spectrum and TAC spectrum as obtained from the coincidence mode data in this experiment.

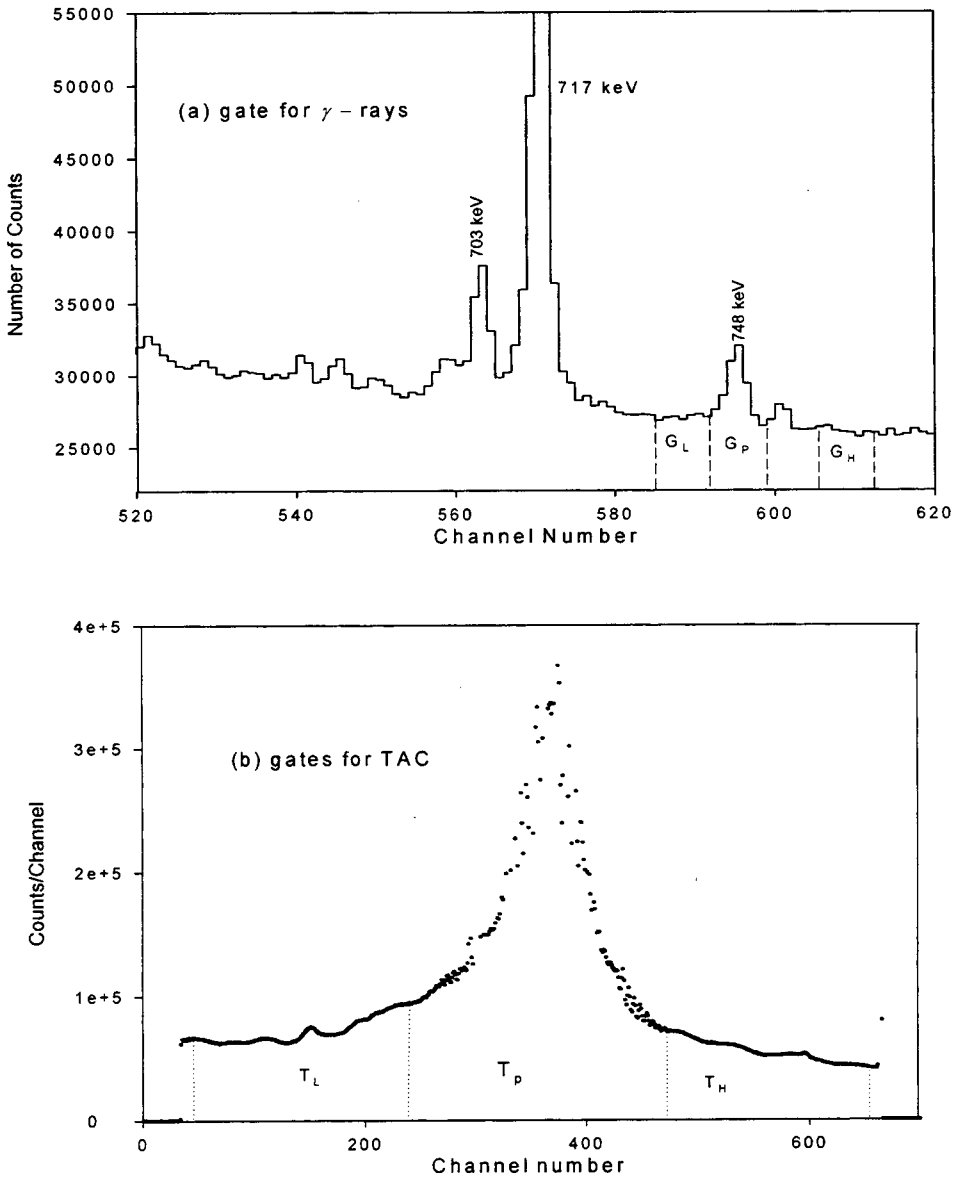

Fig. 5 Gates applied on a). γ-ray energy; and b) TAC spectrum to obtain the true coincidence counts

For this setting, a gated spectrum will be observed. In the same way, the gated spectra for all intense γ-rays over all runs were performed and then summed to obtain the peak area. After then the relative intensities for the cascading γ-lines were determined using the equation:

$$\text{Relative intensity} = I'_{\gamma} = \frac{P_c}{\varepsilon_{\gamma 1}.\varepsilon_{\gamma 2}} \cdot \frac{1}{A.T'} \tag{2}$$

Where, P_c is the coincidence true peak count of the gated spectra for a particular energy, $\varepsilon_{\gamma 1}.\varepsilon_{\gamma 2}$ is the product of efficiencies of two coincident γ-lines, and the term A for activity and T' for measurement time were considered as constants. In order to extract the true coincidence peaks, the procedures for the subtraction of Compton scattering from the γ-ray and the accidental coincidence events from TAC data have been described (Ref. 11, 12). Following the notations such as G_P, G_L and G_H on γ-ray data and T_P, T_L and T_H on TAC data as shown in Fig. 3, the formula for the true counts P_c is given by:

$$P_c = N(G_P,T_P) - R\frac{N(G_L,T_P)+N(G_H,T_P)}{2} - \frac{N(G_P,T_L)+N(G_P,T_H)}{2} + R\frac{N(G_L,T_L)+N(G_H,T_H)}{2} \tag{3}$$

where, $N(G_i,T_j)(i=j=P,L,H)$ stand as the number of counts for 'peak', 'lower' and 'higher' side of the γ-ray gates G_i and TAC gates T_j to the data, respectively. The ratio R is the width for γ peak gate (G_P) to that for off-peak gate $(G_i,(i=L,H))$.

The relative intensities obtained by using Eq. (2) are the observed one where the angular correlation between two γ-rays exist. To find the true relative intensities, it is necessary to make a correction for this effect. The angular correlation between two cascading γ -rays was calculated by the equation:

$$\omega(\theta) = 1 + A_{22}P_2(\cos\theta) + A_{44}P_{44}(\cos\theta) \tag{4}$$

where, the above equation has been derived from the most convenient form as:

$$\omega(\theta) = \sum_{k=0}^{k_{\max}} A_{k_{\max}.k_{\max}.}P_{k_{\max}.}(\cos\theta), \text{ where, } A_{k_{\max}.} = \text{Min}(2I, 2L_1, 2L_2) \tag{5}$$

The term $P_2(\cos\theta)$ and $P_4(\cos\theta)$ are given by:

$$P_2(\cos\theta) = \frac{1}{2}(3\cos^2\theta - 1) \text{ and } P_4(\cos\theta) = \frac{1}{8}(35\cos^4\theta - 30\cos^2\theta + 3) \quad (6)$$

The coefficients A_{22}=A_{44}=A_{kk} were calculated as: $A_{kk} = F_{kk}(L_1 L_1 I_i I)(F_{kk} L_2 L_2 I_f I)$

where, the coefficient values F_{kk}'s were taken from the literatures [7,8], considering the difference of angular momentum, the initial, final and the intermediate spin information. For γ-rays whose multi-polarities are not known, angular correlation between them were assumed to be isotropic. After making the correction for the angular correlation, the corrected relative intensities I_γ can be written as,

$$I_\gamma = I'_\gamma \cdot \frac{1}{\omega(\theta)} \quad (7)$$

With the help of Eq. (2), the above equation becomes,

$$I_\gamma = \frac{P_c}{\varepsilon_{\gamma 1} \cdot \varepsilon_{\gamma 2}} \cdot \frac{1}{\omega(\theta)} \cdot \frac{1}{A.T'} \quad (8)$$

3.3 Determination of cross-section

The rate of reaction produced on ^{105}Pd target can be obtained from the singles spectrum as,

$$\text{Reaction rate} = R_{pd} = \frac{Y}{T_m \cdot \varepsilon_{\gamma pd} \cdot I_{\gamma pd}} \quad (9)$$

Where,

Y = Accumulation of peak counts in a measured time T_m

$\varepsilon_{\gamma pd}$ = Efficiency for a specific energy of ^{106}Pd

$I_{\gamma pd}$ = Gamma-ray intensity for the particular energy obtained from the γ-γ coincidence measurement.

The capture cross section σ_{pd105} of ^{105}Pd can be expressed in terms of reaction rate R_{pd}, neutron flux ϕ (cm^{-2}.s^{-1}) and the number of atoms N_{pd105} present in the target as:

$$\sigma_{pd105} = \frac{R_{pd}}{N_{pd105}.\phi} \tag{10}$$

If the irradiation time is very long compared to the half-life (2.2414±0.0012 min)[1] of ^{28}Al, the activity for the same will attain at saturation region and its amount for the 1779 keV strong γ-line is given by:

$$A_{Al28} = N_{Al}.\sigma_{Al27}.\phi \tag{11}$$

where, the neutron capture cross-section of ^{27}Al becomes,

$$\sigma_{Al27} = \frac{A_{Al28}}{N_{Al27}.\phi} \tag{12}$$

If C be the net counts of a full energy peak for a counting time t_c, then

$$C = A_{Al28}.\varepsilon_{\gamma Al}.I_{\gamma Al}.t_c \tag{13}$$

and, $$A_{Al28} = \frac{C}{t_c.\varepsilon_{\gamma Al}.I_{\gamma Al}} \tag{14}$$

Dividing Eq. (10) by Eq. (12), we obtain:

$$\frac{\sigma_{pd105}}{\sigma_{Al27}} = \frac{R_{pd105}}{A_{Al28}}.\frac{N_{Al27}}{N_{pd105}} \tag{15}$$

which is the required equation for the determination of capture cross-section of ^{105}Pd (σ_{pd105}) relative to the known cross-section of ^{27}Al (σ_{Al27} = 0.231±0.003 barn)[1]. The derived above equation is independent of neutron flux ϕ. The ratio between the number of atoms N_{Al27} and N_{pd105} for both monitor and target, respectively were determined as follows:

The number of atoms per cubic cm in Al = N'_{Al} = density x Avo. Number/ At. Wt.

$$= 2.7 \times 6.02 \times 10^{23} / 26.98 \approx 6.024 \times 10^{22} \text{ nuclei/cm}^3$$

The number of atoms for Al containing the volume V_{Al} (= S. t_{Al}) is:

$$N_{Al27} = N'_{Al} . V_{Al} = N'_{Al} . S. t_{Al} \quad (16)$$

where, S is the area in beam interacting position and t_{Al} is the thickness of the monitor.

As above, the number of atoms of ^{105}Pd per cubic cm present in Natural Pd is:

N'_{pd105} = Density . Avo. Number. Isotopic abundance / At. Wt.

= 12.02 x6.02 x10^{23}x0.2233 / 106.42 = 1.52 x10^{22}

and N'_{pd105} = 6.38 x10^{22} for enriched ^{105}Pd with an enrichment of 93.8%.

The number of atoms of ^{105}Pd in the volume V_{pd} containing the same area S as for Al and the target thickness t_{pd} is:

$$N_{pd105} = N'_{pd105} . V_{pd} = N'_{pd105} . S. t_{pd} \quad (17)$$

Dividing Eq. (16) by Eq. (17) yields,

$$\frac{N_{Al27}}{N_{pd105}} = \frac{N'_{Al}}{N'_{pd105}} . \frac{t_{Al}}{t_{pd}} \quad (18)$$

The above equation is the ratio between the numbers of atoms of Al to the target ^{105}Pd, which is proportional to the ratio of the corresponding sample thickness, respectively.

4. Results and Discussion

The results of the present study can be presented as:

- Partial level-scheme
- Relative γ-ray intensities
- Capture cross-sections

4.1 Partial level-scheme

A portion of singles γ-ray spectrum of ^{106}Pd for both natural Pd and enriched ^{105}Pd marked with γ-lines are shown in **Figure 6 (a)** and **(b)**, respectively. The identified γ-lines from the natural Pd have confirmed with the spectrum of Enriched ^{105}Pd.

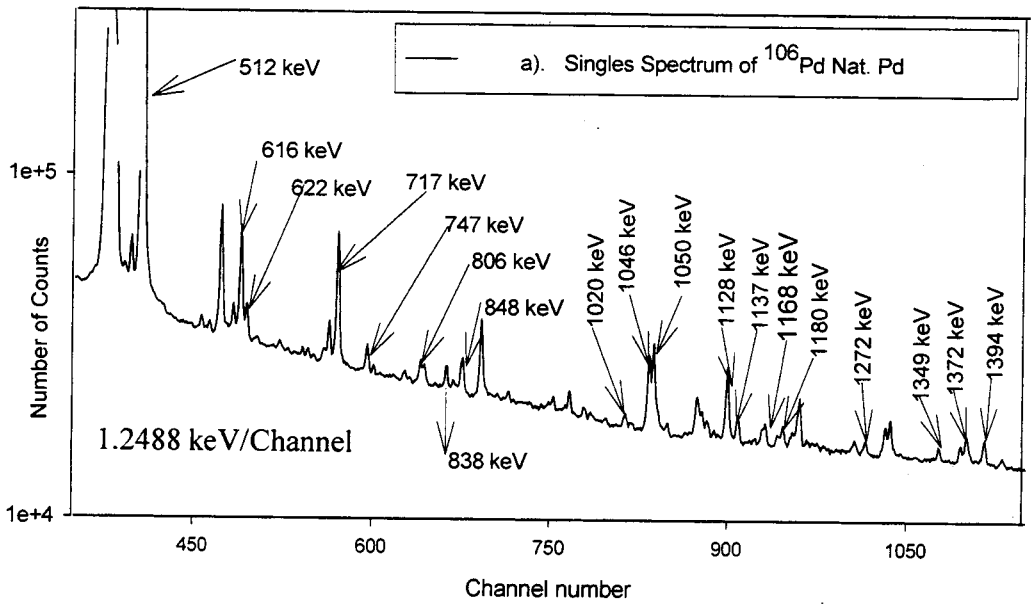

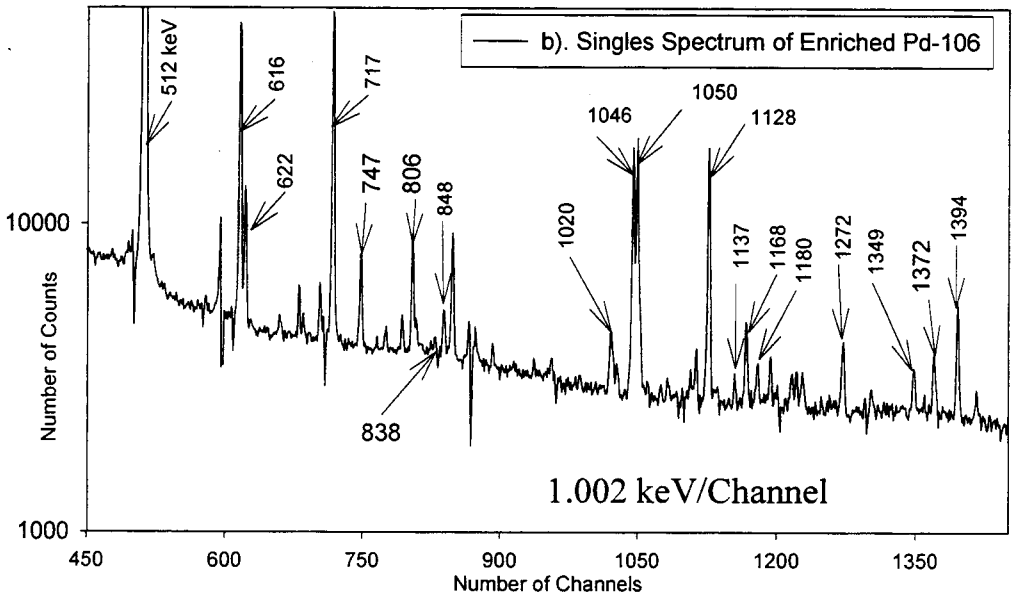

Fig. 6 Singles γ-ray spectrum of ^{106}Pd; a) captured by the natural Pd, b). captured by the enriched ^{105}Pd

The procedure for the creation of gated spectra has already been described elsewhere in this text. It will contain a large volume to accommodate all of them and as such as, we have planned to display only a few of them as an illustration shown in **Figure 7**. The results of coincident γ-transitions for the corresponding gates are summarized in **Table 1**. In the present investigation, about 20 gated spectra were created and more than 40 γ-lines were allowed to construct the partial level-scheme. The partial level-scheme is shown in **Figure 8**. Here, two levels at 1906 and 2400 keV (dot lines in Fig. 8) are identified as new levels. The level at 1906 keV has been assigned by observing the 512 keV line gated by 1394 keV line and vice-versa (shown in Fig. 7. (a) and (b)). Another level at 2400 keV has been confirmed by observing the transitions 512 and 1050 keV; and 512 and 838 keV gated by 838 and 1050 keV, respectively as shown in Fig 7 (c) and (d). No γ-transitions was observed from the capturing state.

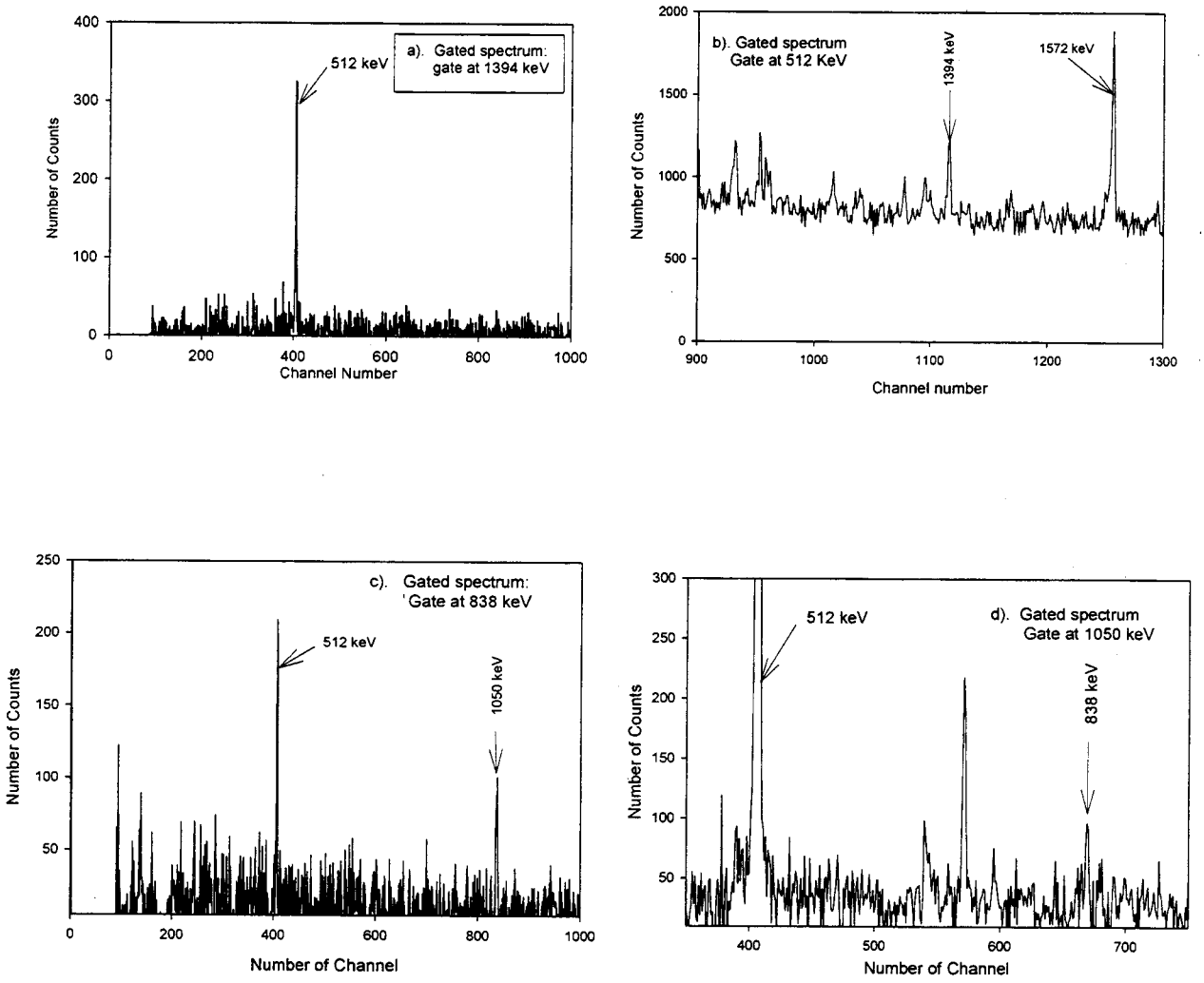

Fig. 7 Coincidence gated spectra for; a). gate at 1394 keV; and b). gate at 512 keV, c) gate at 838 keV, and d) gate at 1050 keV

Table 1 Coincident γ-transitions in ^{106}Pd

Gate applied at energy (keV)	Coincident γ-transitions in (keV)
512	430, 616, 622, 680, 685, 703, 717, 748, 792, 804, 808, 838, 848, 874, 956, 1046, 1050, 1114, 1137, 1168, 1195, 1180, 1223, 1272, 1349, 1394, 1498, 1572, 1649, 1797, 1929, 1988, 2271, 2234, 2457.
616	430, 512, 748, 804, 874, 956, 1114, 1180, 1223, 1272, 1372, 1498
622	428, 512, 1108
717	512, 703, 848, 1054, 1137, 1168, 1349, 1649
748	430, 512, 616, 1046
804	512, 616, 1128
808	512, 1046
838	512, 1050
848	512, 717
1046	512, 586, 685, 748, 792, 808, 1020
1050	512, 680, 716, 838
1128	430, 512, 804, 874, 1181
1181	512
1272	512, 616
1349	512, 717
1394	512
1572	512
1797	512

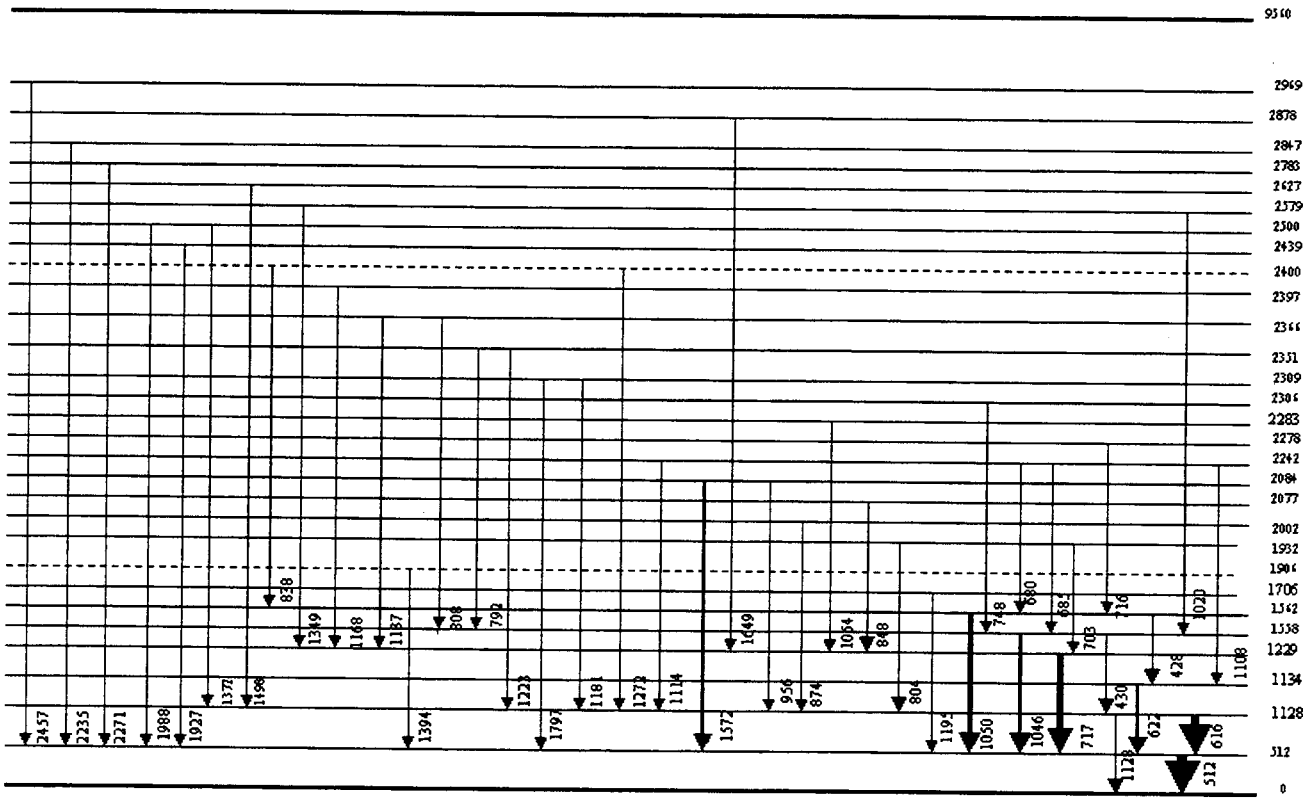

Fig. 8 Partial level -scheme of ^{106}Pd , the dot lines are new levels and the thick solid line (upper) is the capturing state

4.2 Relative γ-ray Intensities

By inserting the values of the product of efficiencies of two coincident γ-lines and the true coincidence peak counts, the relative intensities have been calculated by Eq. (7). The final intensity values were calculated by averaging all the individual intensities for the same energy point obtained by imposing gates at various transitions. The measured coincidence relative intensities in percent of the total observed γ-lines feeding to the different levels are shown in **Table 2**. From this Table, it is observed that the weak intensity γ-lines has the highest uncertainty. The uncertainty at 1046 and 1050 keV is comparatively high due to the overlapping of two closely spaced peaks though both of them are intense. In reality, it is very difficult to separate two

closely peaks if they are out of detector resolution limits and the measured intensities will not be in accurate. For the same reason, we are not able to use the 512 keV strongest γ-peak because of its superposition with the annihilation peak of 511 keV.

Table 2 Measured relative γ-ray intensities in percent of the total

Level at keV	Coincidence γ-transitions in keV	Relative intensities with errors in %
512	616	20.30±0.78
	622	3.74±0.52
	717	25.06±1.43
	1046	13.86 ±1.94
	1050	13.26 ±2.52
	1195	1.12±0.15
	1394	2.63±0.33
	1572	9.42±0.24
	1797	1.30±0.18
	1927	2.04±0.29
	1988	2.54±0.35
	2271	0.74±0.10
	2234	1.77±0.25
	2457	2.17±0.30
1128	430	3.09±0.48
	804	1.81±0.44
	874	0.74±0.41
	956	0.42±0.06
	1114	0.39±0.05
	1181	0.16±0.02
	1223	0.46±0.10
	1272	1.34±0.20
	1372	1.27±0.30
	1498	1.41±0.69
1134	428	0.53±0.07
	1108	0.60±0.08
1229	703	1.02±0.02
	848	3.13±0.36
	1054	1.61±0.23
	1137	0.30±0.04
	1168	3.00±0.66
	1349	0.67±0.08
	1649	0.69±0.10
1558	685	0.46±0.11
	748	2.39±0.48
	792	0.84±0.28
	808	0.90±0.27
	1020	0.46±0.06
1562	716	1.42±0.19
	680	0.92±0.13
	838	0.98±0.09
0	512	95.04±1.54
	1128	4.96±0.28

4.3 Determination of cross-sections

The capture cross-sections for both natural and enriched ^{105}Pd were determined by Eq. (15) and the results are given below:

i) Cross-sections for natural Pd

The ratio of number of atoms between Al and the target ^{105}Pd was determined following Eq. (18), giving the thickness values of t_{Al} and t_{pd} are 0.024 and 0.0126 cm, respectively. Thus, $\frac{N_{Al27}}{N_{pd105}} = 7.54$

The reaction rates of ^{105}P (R_{pd105})and the activity for the 1779 keV γ-line of ^{28}Al at saturation region (A_{Al28}) are shown in **Table 3 (a)** and **(b)**, respectively.

The capture cross-section for the natural Pd is:

σ_{pd105} = 8.80 ± 0.59 (6.77%) barn

Table 3(a) Reaction rates of ^{105}Pd for the natural Pd target

Run No.	Energy in keV	Peak count rate* $(\frac{Y}{T})$	Efficiency $=\varepsilon_\gamma$ x10 $^{-2}$	Gamma emission (I_γ) in %	Reaction Rate R	Weighted mean
1	616	20.39±2.37%	0.848 ±1.97%	20.30 ±0.78	11844.73±4.93%	11690.80±4.93%
	717	21.08±2.07%	0.736 ±1.93%	25.06± 1.43	11429.09±6.37%	
	1046	7.57±3.93%	0.519 ±1.90%	13.86± 1.94	10523.62±14.68%	
	1050	8.78±3.51	0.517 ±1.90%	13.26±2.51	12807.38±19.38%	
	1572	3.99±6.37%	0.355 ±1.96%	9.42 ±0.24	11931.46±7.16%	
2	616	19.53 ±2.19%	〃	〃	11345.15±4.84%	11254.74±4.84%
	717	22.34 ±1.94%	〃	〃	124106.81±6.33%	
	1046	7.80 ± 3.63%	〃	〃	10843.36±14.60%	
	1050	7.89 ±3.44%	〃	〃	11509.14±19.37%	
	1572	3.51±5.56%	〃	〃	10496.10 ±6.43%	
3	616	19.86±2.08%	〃	〃	11536.85±4.79%	11413.64±4.79%
	717	23.00±1.93%	〃	〃	12470.07±6.33%	
	1046	7.39±3.87%	〃	〃	10273.39±14.67%	
	1050	8.54±3.46%	〃	〃	12457.30±19.37%	
	1572	3.51±5.96%	〃	〃	10496.10±6.78%	
4	616	20.90±2.24%	〃	〃	12141.00±4.87%	11515.76±4.87%
	717	21.10±2.07%	〃	〃	11439.93±6.37%	
	1046	7.37±3.85%	〃	〃	10245.59±14.66%	
	1050	9.05±3.31%	〃	〃	13201.23±19.35%	
	1572	3.62±5.76%	〃	〃	10825.03±6.60%	
5	616	20.99±2.09%	〃	〃	12193.28±4.78%	12284.85±4.78%
	717	21.35±2.01%	〃	〃	11575.48±6.35%	
	1046	7.88±3.62%	〃	〃	10954.58±14.60%	
	1050	8.53±3.27%	〃	〃	12442.71±19.3%	
	1572	4.59±5.22%	〃	〃	13725.67±6.12%	
mean						11613.51±4.78%

Table 3(b) Saturated activity of 1779 keV γ-ray of ^{28}Al

Run No.	Count-rate*	Efficiency	Activity	Weighted mean
1	7.24±4.58%	0.309x10^{-2}±2.0%	2283.91±5.0%	
2	7.48±4.15%	〃	2359.62±4.61%	2298.98±4.61%
3	7.14±4.36%	〃	2252.36±4.80%	

* Count -rates were taken after the subtraction of background for the same measurement time.

ii) Capture cross-section for enriched ^{105}Pd

The thickness of t_{Al} and t_{pd} for Al and enriched ^{105}Pd are 0.0118 and 0.00058 cm, respectively and the atomic ratio is:

$$\frac{N_{Al27}}{N_{pd105}} = 19.21$$

The rate of reaction for enriched ^{105}Pd and the saturation activity of ^{28}Al are shown **in Table 4 (a)** and **(b)**, respectively

The capture cross-section is found to be $\sigma_{pd105} = 9.53 \pm 0.47$ (4.95%) barn.

From the cross-section values as above, it shows that the value of natural Pd is lower than that of enriched one, but they coincide within the error limits to each other. As the presence of impurities in the natural Pd sample is comparatively higher than the enriched sample and there is a possibility to deteriorate the cross section for the former one. To determine the reliable cross-section, it is necessary to use the absolute emission probabilities. In order to do so, the contribution for missing transitions will be taken in to account very carefully.

Table 4(a) Reaction rates for the enriched ^{105}Pd sample

Run No.	Energy in keV	Peak count rate* $(\frac{Y}{T})$	Efficiency = ε_γ x10 $^{-2}$	Gamma emission (I_γ) in %	Reaction Rate R	Weighted mean
1	616	19.69 ± 0.98%	1.352 ± 1.93%	20.30 ± 0.78	7174.19 ± 4.41%	7249.51 ± 4.41%
	717	22.93 ± 0.88%	1.188 ± 1.92%	25.06 ± 1.43	7702.05 ± 6.09%	
	1046	8.00 ± 1.68%	0.860 ± 1.92%	13.86 ± 1.94	6711.63 ± 14.25%	
	1050	9.96 ± 1.48%	0.857 ± 1.92%	13.26 ± 2.51	8764.66 ± 19.12%	
	1572	4.08 ± 2.74%	0.607 ± 1.93%	9.42 ± 0.24	7135.44 ± 4.21%	
2	616	19.98 ± 0.48%			7279.85 ± 4.33%	7152.61 ± 4.33%
	717	23.52 ± 0.45%			7900.23 ± 6.04%	
	1046	7.99 ± 0.82%			6703.24 ± 14.16%	
	1050	9.26 ± 0.74%			8148.67 ± 19.08%	
	1572	3.94 ± 1.45%			6890.59 ± 3.51%	
3	616	20.76 ± 0.39%			7564.05 ± 4.32%	7337.63 ± 4.32%
	717	23.97 ± 0.35%			8051.38 ± 6.04%	
	1046	8.45 ± 0.68%			7089.16 ± 14.16%	
	1050	9.91 ± 0.61%			8720.66 ± 19.07%	
	1572	4.02 ± 1.12%			7030.50 ± 3.39%	
mean						7245.22 ± 4.32%

Table 4 (b) Saturated activity for the 1779 keV γ-line of ^{28}Al

Run No.	Count-rate*	Efficiency (X10^{-2})	$I_{\gamma Al}$	Activity	Weighted mean
1	18.30 ± 1.02%	0.546 ± 1.93%	100%	3351.65 ± 2.18%	3371.98 ± 2.01
2	18.51 ± 0.56%	,,	,,	3390.11 ± 2.01%	

* Count -rates were taken after the subtraction of background for the same measurement time

5. Conclusions

In the present investigation, the partial level-scheme of ^{106}Pd was studied with thermal neutrons by the (n,γ) reaction. On the basis of this level-scheme, the relative γ-ray intensities were measured from the γ-γ coincidence data and a few of intense γ-lines were used to derive the cross-sections for the reaction. As a whole, the present study concludes as follows:

- The relative intensities for the ^{14}N(n,γ)^{15}N reaction was deduced.
- The partial level-scheme of ^{106}Pd was obtained, and two new levels were identified in this level-scheme.

Acknowledgements

The authors would like to thank to the technical staff at KURRI for their cooperation during the irradiation of samples. The author (M.M.H. Miah) is very grateful to the Japan Science and Technology (JST) for providing a fellowship to perform this work.

REFERENCES

1. R.B. Firestone, V.S. Shirley, C.M. Baglin, S.Y. F. Chu and J. Zipkin, *Table of Isotopes*, 8th edition., John Wiley & Sons, New York, (1998).

2. J. Katakura, *Chart of the Nuclides*, Nuclear Data Center, JAERI, Tokai-mura, Japan (2000).

3. R.L. Macklin, J. Halperin and R.R. Winters, "$^{104, 105, 106,108,110}$Pd (n,γ) Cross Sections above 2.6 keV", *Nucl. Sci. & Eng.*, **71**, 182 (1979).

4. ENDF, 1999. Evaluated nuclear structure data file—a computer file of evaluated experimental nuclear structure data maintained by the National Nuclear Data Center, *Brookhaven National Laboratory*; http://www.nndc.bnl.gov/nndc/ensdf/.

5. K. Debertin, U. Schotzig, "Coincidence summing corrections in Ge(Li)-spectroscopy at low source-detector distances", *Nucl. Instrum. Methods*, 158, 471, (1979).

6. H. Frauenfelder and R.M. Steffen, "*Angular Correlations", (Alpha-, Beta- and Gamma – Ray spectroscopy*, ed. By K. Siegbahn), Vol. 2, 997- 1198, (1968).

7. H. Morinaga and T. Yamazaki, "*In-beam Gamma-Ray Spectroscopy*", North –Holland Publishing Company, Amsterdam, 81-103, (1976).

8. T.J. Kennett, W.V. Preswich, J.S. Tsai, *Nucl. Instr. & Meth.* A249, 366, (1986).

9. E.T. Jurney, J.W. Starner, J.E. Lynn, S. Raman, *Phy. Rev.* C56, 118, (1997).

10. K. Furutaka, S. Nakamura, H. Harada, T. Katoh, T. Fuji and H. Yamana, "Precise measurement of Gamma-ray Emission Probabilities of ^{100}Ru", *J. Nucl. Sci. Technol.*, 38(12), 1035, (2001).

11. K. Furutaka, S. Nakamura, H. Harada and T. Katoh, "Evaluation of β-γ Coincidence Measurement System Using Plastic Scintillation β-ray Detector Developed for the Determination of γ-ray Emission Probabilities of Short-lived Nuclides", *J. Nucl. Sci. Technol.*, **37**, 832, (2000).